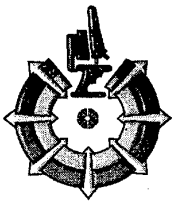

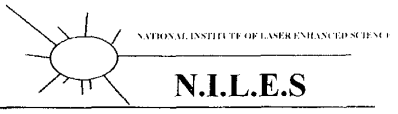

Effect of Synthecizers on the Optical Properties of Er^{3+} Ions in Erbium Glass Lasers

A.M. ABDEL SATTAR, I.M.Azzouz,
M. Salah Shafik, and Y.A. BADR

National Institute of Laser Enhanced Sciences,
Cairo University, Cairo, Egypt

Effect of Synthecizers on the Optical Properties of Er^{3+} Ions in Erbium Glass Lasers

A.M. ABDEL SATTAR, I.M.Azzouz,

M.Salah Shafik, and Y.A. BADR

National Institute of Laser Enhanced Sciences, Cairo University,

Cairo,Egypt.

Abstract

Two different host glasses for Er^{3+}, namely, phosphate and borate glasses were prepared. Yb^{3+} was added as a sensitizer to investigate its effect on the absorption, emission, gain cross sections as well as threshold pumping intensity for generation of laser radiation. Another sensitizer, Cr^{3+}, was added to Er^{3+}.The enhancement of absorption and emission of Er^{3+} were investigated, in addition, the energy transfer efficiency from Cr^{3+} to Er^{3+} was determined from the emission of Cr^{3+}. The threshold intensity for Er^{3+} laser at 1543 nm is reduced to about 54 times using Yb^{3+} as a sensitizer.

1. Introduction

The most important feature of erbium glass lasers is its operation in the eye-safe regions at wavelengths near near 1.5 μm. Lasing characteristics such as pumping efficiency,laser threshold and intrinsic slope efficiency have been reported in Er:Yb glasses and crystals[1-9].by contrast there are only a few spectroscopic measurements for these ions. However it is important to understand the spectroscopy of Er^{3+} singly doped or Er^{3+} co-doped with either Yb^{3+} or Cr^{3+} . There are some spectroscopic properties that are important for this laser. Typical properties are the stimulated emission cross section, upper state lifetime and absorption spectra.In this work, we report the results of spectroscopic measurements for Er^{3+}or Er^{3+} co-doped with either Yb^{3+} or Cr^{3+}in order to assess their potential laser performance and to identify specific candidates for laser operation.

2. Experimental procedure

2.1 Sample preparation

The samples used in this study were prepared with highly purified materials. The mixed chemicals were melted in a highly purified fused quartz crucible to give high quality optical glass in an electric furnace in a temperature range from 1250-1350°C depending on the sample composition for about 1.5 h. Glass samples were cast into a preheated aluminum mold . When the glass had solidified to support itself, it was removed from the mold and transferred to an annealing furnace. Glass samples were annealed for two hours at a temperature from 510-530°C and cooled at room temperature at a rate of 10°C per hour for obtaining high quality optical glass. The composition of the prepared samples is listed in table 1. Many papers reported sample preparation for phosphate and borate glasses [10-15].

2.2 Sample evaluations

Glass sample of 2 mm thick with two polished faces were used for absorption, density, and refractive index measurements. Absorption spectra were measured with double beam spectrophotometer (Perkin Elmer lambda 40). An undoped sample with the same thickness was placed in the reference beam in order to eliminate the influence of intrinsic absorption for the host material. The absorption cross section for Er^{3+} singly-doped is given by [13]

$$\sigma_{ab} = \frac{2.303}{Nl} A \qquad (1)$$

Where A is the absorbance of Er^{3+}, l is the the thickness of the sample, and N is the Er^{3+} concentration. The number of the active ions per cm^3 was determined from the concentration in the starting mixture and the sample density. This has been found to be accurate for the previous rare earth dopiness of oxide glasses [16], [17], and [18]. In case of sensitizing Er^{3+} with Cr^{3+} or Yb^{3+} the effective absorption cross-section of Er^{3+} is also given by (1) with A stands for the effective absorbance. Density was determined by Archimedes method using xylene as an immersion liquid. Refractive indexes were measured at 532, 543.5, 632.8, and 1064 nm using Brwester method. The Caushy dispersion equation was used to determine the refractive index at other wavelengths.

Fluorescence spectra were measured with a laser diode (Model L. M. 2500 Applied Optoronics) as a pumping laser (centered at 980 nm). This line matches $^4I_{11/2}$ - $^4I_{15/2}$ transition of Er^{3+} which lies in close to $^2F_{7/2}$ - $^2F_{5/2}$ transition of Yb^{3+}. A non-radiative transition occurs from $^4I_{11/2}$ to $^4I_{13/2}$ followed by radiative transition occurs from $^4I_{13/2}$ to $^4I_{15/2}$ at 1534 nm. The pumping laser was chopped at 15 Hz and incident on the sample. The emission from the sample was focused on a monochromator (Spex

Industeries, INC. Model 750 M) and detected by an InGaAs detector. The signal was amplfied with a lock-in amplifier and displayed by a computer. The resolution of the system was 0.4 nm.

Similar data acquisition was performed for the lifetime measurement of $^4I_{13/2}$ state. Luminescence decay curves were recorded and averaged by a digital osciloscope system.

The stimulated emission cross-section was scaled using the emission line shape function with peak emission cross section being scaled by [19]

$$\frac{1}{\tau} = \frac{8\pi^2 n^2}{c^2} \int \upsilon^2 \sigma_{em} \, d\upsilon \qquad (2)$$

Where τ is the $^4I_{13/2}$ lifetime.

3. Experimental results

3.1 absorption spectra

Fig.1(a),(b) shows the absorption spectra of Er^{3+} singly-doped and Er^{3+}:Yb^{3+} doubly doped in phosphate glass respectively. In case of sensitizing Er^{3+} with Yb^{3+}, there is a strong absorption band at 980 nm due to $^2F_{7/2}$ -$^2F_{5/2}$ transition of Yb^{3+}. Fig1(c) shows the absorption spectra of Er^{3+}: Cr^{3+} doubly-doped. The two broad bands centered at 650 and 450 nm are due to $^4A_2(t_2^3) \rightarrow {}^4T_2(t_2^2 e)$ and $^4A_2(t_2^3) \rightarrow {}^4T_1(t_2^2 e)$ respectively. These two broad bands of Cr^{3+} make Er^{3+} glass laser more efficient in case of pumping with a flash lamp. Fig.1(d) shows the absorption spectra of Er^{3+}:Yb^{3+} in borate glass.

3.1.1 Optical properties and Judd-Ofelt analysis

The measured line strength of the absorption transition from a level J to a level J' is related to the integrated absorption cross-section:

$$\int \sigma d\lambda = \frac{8\pi^3 \bar{\lambda}}{3ch(2J+1)} (\chi_{ed} S_{ed} + \chi_{md} S_{md}) \qquad (3)$$

where c is the velocity of light, $\int \sigma d\lambda$ is the integrated absorption cross section, n is the refractive index of the sample, and the χ terms are defined as

$$\chi_{ed} = n(n^2+2)^2/9 \qquad (4)$$

for electric dipole transition and

$$\chi_{md} = n^3 \qquad (5)$$

for magnetic dipole transition.. The calculated line strength of electric and magnetic dipole transitions S_{ed} and S_{md} between initial manifold ψJ and terminal manifold $\psi' J'$ are expressed as.

$$S_{ed} = e^2 \sum_{\lambda=2,4,6} \Omega_\lambda (\Psi J \| U^\lambda \| \Psi' J')^2 \qquad (6)$$

and

$$S_{md} = e^2 h^2 / 16\pi^2 m^2 c^2 (\psi J \| L + 2S \| \psi' J')^2 \qquad (7)$$

The matrix elements U^λ and $L+2S$ in the above equations are calculated using formulas given elsewhere. In this work the matrix elements calculated by Weber [20] for Er^{3+} in LaF_3 have been used. This is reasonable since the matrix elements are almost host invariant. The calculated line strength of the magnetic dipole transition was subtracted from the total line strength of the absorption bands containing electric and magnetic dipole transitions. The optimum combination of Judd-Offelet parameters Ω_t with t=2,4,6 in phosphate glass was determined by a least square-fitting between measured and calculated line strengths to find the calculated values of Ω_t

$\Omega_2 = 8.65 \times 10^{-20} cm^2, \Omega_4 = 1.95 \times 10^{-20} cm^2, \Omega_6 = 1.77 \times 10^{-20} cm^2.$

The measured and calculated line strength for Er^{3+} in phosphate glass is shown in table (2).A magnetic dipole transition makes a significant contribution only to the

$^4I_{15/2} \rightarrow {}^4I_{13/2}$ transition. Thus, this transition had to be omitted when fitting the Judd-Ofelt parameters. All other transitions are electric dipole in nature.

The radiative decay probability from certain state u to the ground state g is measured from the absorption spectrum using the formula

$$A_u = 8\pi c \frac{n^2 g_g}{\bar{\lambda}^4 g_u} \int \sigma d\lambda \qquad (8)$$

Where;

$\bar{\lambda}$ is the mean absorption wavelength, g_g is the degeneracy of the ground state, g_u is the degeneracy of the upper state, and $\int \sigma d\lambda$ is the integrated absorption cross section. Another formula to the radiative transition probability is

$$A_u = \frac{64\pi^4}{3h\bar{\lambda}^3(2J+1)} \times \left[(n(n^2+2)^2/9) S_{ed} + n^3 S_{md} \right] \qquad (9)$$

The total radiative transition probability for an excited state is given as the sum of the $A(\Psi J, \Psi' J')$ terms calculated over all terminal states which is related to the radiative lifetime, τ_R, and the branching ratio β, of the level by

$$A_T(\Psi J) = \sum_{\Psi' J'} A(\Psi J, \Psi' J') \qquad (10)$$

$$\beta_R(\Psi J, \Psi' J') = [A(\Psi J, \Psi' J')] / A_T(\Psi J) \qquad (11)$$

$$\tau_R(\Psi J) = [A_T(\Psi J)]^{-1} \qquad (12)$$

The values of A_{ed}, A_{md}, and β_R for Er^{3+} ions in phosphate glass are shown in table (3).

Similarly for Er^{3+} ions in borate glass. Table (4). shows the measured and calculated line strength for some Er^{3+} energy levels.

The optimum combination for $\Omega_2, \Omega_4, \Omega_6$ is

$\Omega_2 = 4.26 \times 10^{-20} cm^2, \Omega_4 = 1.7 \times 10^{-20} cm^2, \Omega_6 = 3 \times 10^{-21} cm^2$

The values of A_{ed}, A_{md}, and β_R for Er^{3+} ions in borate glass are shown in table (5).

3.2 Fluorescence spectra

Fig.(2) shows the effect of Er^{3+} concentration on the fluorescence lifetime of $^4I_{13/2}$ in phosphate glass. It is clear that as the concentration increases, self-quenching for emission increases, which yields to a decrease in the fluorescence lifetime of $^4I_{13/2}$ of Er^{3+} [21].

The stimulated emission cross-sections of Er^{3+} singly-doped and Er^{3+}: Yb^{3+} doubly-doped are shown in fig.(3). Clearly, the Yb^{3+} enhanced the stimulated emission cross section at 1534 nm, by non-radiative energy transfer process through dipole-dipole interaction mechanism.

There is a strong matching between the exciting diode laser and the absorption of Yb^{3+}, fig(4).

Fig(5) shows the effect of Cr^{3+} as a sensitizer on the stimulated emission cross section of Er^{3+} at 1534 nm . Cr^{3+} did not enhance the stimulated emission cross section of Er^{3+} at 1534 nm.This is due to the fact that no matching between the diode laser line and the absorption of Cr^{3+}, Fig(6).The effect of the host glass on the stimulated emission cross-section of Er^{3+}:Yb^{3+} doubly-doped is shown in fig.(7).In phosphate glass, there is strong matching between $^2F_{5/2}$ state of Yb^{3+} and $^4I_{11/2}$ state of Er^{3+};yields higher stimulated emission cross section of Er^{3+} in phosphate glass.

A very important parameter in laser physics is the gain cross-section. It is defined as

$$G(\lambda) = \beta\sigma_{se} - (1-\beta)\sigma_{ab}$$

Where β is the pumping parameter, $\beta = \frac{N_e}{N}$ where N_e is the population of Er^{3+} in the excited state, and N is the total concentration of Er^{3+}. β depends on the pumping

power. Using the simple rate equations of Er^{3+}, $N_e = 2.8\times10^{17}$ ions/cm^3 and $\beta = 0.028$. In case of Er^{3+}:Yb^{3+},due to efficient energy transfer process from Yb^{3+} to Er^{3+}, the population of Er^{3+} (calculated using wright equation; stating that the population in the upper state is proportional to the fluorescence intensity) in the $^4I_{13/2}$ is 3.77×10^{18} ions/cm^3, yields $\beta = 0.377$. Fig(8) shows the gain cross-section of Er^{3+} singly-doped and Er^{3+}: Yb^{3+} doubly-doped. A very important parameter in sensitization process is the transfer efficiency [22-24]. It is defined as

$\eta = 1 - \frac{I}{I_0}$ where I, I_0 are the emission intensity of sensitizer with and without activator, respectively. To measure transfer efficiency from Cr^{3+} to Er^{3+}, samples containing Cr^{3+} are excited by He-Ne laser (632.8 nm). This wavelength matches $^4A_2(t_2^3) \rightarrow {}^4T_2(t_2^2 e)$ transition in Cr^{3+}. Non-radiative transition occurs from $^4T_2(t_2^2 e)$ to ^2E state, followed by radiative transition from ^2E state to $^4A_2(t_2^3)$ centered at 810 nm. The fluorescence of Cr^{3+} singly-doped and Cr^{3+}: Er^{3+} doubly-doped in phosphate glass is shown in Fig. (9). Before sensitization occurs, the population of Cr^{3+} in the ^2E state is high, thus the fluorescence intensity is high. But in the presence of Er^{3+} most of the population of Cr^{3+} in the ^2E state is transferred to $^4I_{9/2}$ Er^{3+}.

4. Discussion

Due to small absorption cross section of Er^{3+} singly-doped at 980 nm is small, consequently the threshold laser intensity (for zero-loss conditions) required to generate Er^{3+} laser at 1534 nm is high

$$I_{th} = \frac{hc}{\sigma_{ab}\lambda_p \tau}$$

where λ_p is the pumping wavelength=980 nm, $\sigma_{ab} = 2\times 10^{-20}$ cm^2, 6.13 ms so the threshold intensity is 1.65 K.W/cm^2 . On the other hand, when Yb^{3+} is used as a

sensitizer, with the effective absorption cross-section 1.08×10^{-18} cm^2, the threshold intensity was 30.5 W/cm^2. This means that the threshold intensity is reduced to about 54 times. The $^2F_{5/2}$ state of Yb^{3+} serves as a store of population for $^4I_{13/2}$ of Er^{3+} to provide the necessary population inversion for Er^{3+} required for laser. The efficient energy transfer process from Yb^{3+} to $Er^{3+}$is enhancing the gain cross section at 1534 nm from negative values to positive ones.

The two broad bands of Cr^{3+} are suitable for a flashlamp excitation .The transfer efficiency from Cr^{3+} to Er^{3+} at 810 nm is 86%.

5. Conclusion

The absorption, stimulated emission and gain cross-sections for Er^{3+} are enhanced using Yb^{3+} as a sensitizer. The threshold intensity required for 1534 nm Er^{3+} laser is reduced to about 50 times using Yb^{3+} as a sensitizer. The transfer efficiency from Cr^{3+} to Er^{3+} at 810 nm is high; about 86%.

6. Acknowledgement

I am taking a great pleasure to thank Nagia El-Alili ,staff member at Radiation Technology Center for her facilities to prepare my samples.

7. Referrences

[1]- E. Georgious , O. Musset , J.P. Boquillion, High-efficiency and high-output pulse energy performance of a diode-pumped Er:Yb:glass 1.54-μm laser, App.Phys. B, 70 (2000) 755-762.

[2]-Shibin Jiang, Michael Myers, Nasser Peyghambarian, Er^{3+} doped phosphate glasses and lasers, J. Non-Crys.Solids,.239 (1998) 143-148.

[3]- S. Taccheo, P. laporta, S. Longhi, O. Sevelto, C. Svelto, Diode pumped Er^{3+}:Yb^{3+} lasers, Appl. Phys. B, .63 (1996) 425-436.

[4]- T. Schweizer, T. Jensen, E. Heumann, and G. Huber, Spectroscopic properties and diode pumped 1.6 μ m laser performance in Yb co-doped Er: $Y_2Al_5O_{12}$ and Er^{3+} Y_2SiO_5, Opt. Comm., 118 (1995) 557-561 .

[5]-C.Li, R.Moncorgé, J.C. Souriau, C.Borel,Ch.Wyon, Room temperature cw laser action of $Y_2SiO_5:Yb^{3+},Er^{3+}$ at 1.57 μ m, Opt.Comm.,107 (1994) 61-64.

[6]- P. Laporta, S. De Silveestri, V. Magni, and O. Svelto, Diode-pumped cw bulk Er:Yb:glass laser, Optics Letters, 16 (1991) 1952-1954.

[7]- Matjaz Lukac and Marko Marincer, Energy Storage and heat Deposition in Flash Lamp Pumped Sensitized Erbium glass lasers, IEEE, J. Quantum Electronics, 26 (1990) 1779-1785.

[8]- W.L. Barnes, P.R. Morkel, L. Reekie, and D.N. payne, High quantum efficiency Er^{3+} fiber lasers pumped at 980 nm, Opt.Lett., 149, (1989) 1002-1004.

[9]- Jiang Yasi, Zhang Junzhou, Xu Wenjiun, M. A. Zhongtang, Ying Xingxin, Mao Hanfen, Moo Sen and Li Jie, Preparation techniques for phosphate laser glasses, J. Non-Crys. Solids, 80 (1986) 623- 629.

[10]- A. Renuka Devi, C.K. Jayasankar, Optical properties of Er^{3+} ions in lithium borate glasses and comparative energy level analyses of Er^{3+} ions in various glasses, J. Non-Crys. Solids,197 (1995) 111-128.

[11]- Wolfgang Seeber, Doris Ehrt, and Heike Ebendorff- Heideprime, Spectroscopic and laser properties of Ce^{3+}-Cr^{3+}-Nd^{3+} co-doped fluoride phosphate and phosphate glasses, J. Non-Crys. Solids, 171 (1993) 94-104.

[12]-H. Ebendorff- Heidepriem, W. Seeber, and D. Ehrt, Dehydration of phosphate glasses, J. Non-Crys. Solids, 163 (1993) 74-80.

[13]- Hiromichi Takebe, Takehiro Murata, and Kenji Morinaga, Compositional dependence of absorption and fluorescence of Yb^{3+} in oxide glasses, J.Am.Ceram.Soc.,79 (1996) 681-687.

[14]- Yoshikzu Nageno, Hiromichi Takebe, and Kenji Morinaga, Correlation between radiative transition probabilities of Nd^{3+} and composition in silicate,borate, and phosphate, J.Am.Ceram.Soc.,76 (1993) 3081-3086.

[15]-Jiang Yasi, Jiang shibin and Jiang Yanyan, Spectral properties of Nd^{3+} in aluminum phosphate glasses, J. Non-Crys. Solids, 112 (1989) 286-290.

[16]- Hiromichi Takebe, Takehiro Murata, and Kenji Morinaga, Compositional dependence of absorption and fluorescence of Yb^{3+} in oxide glasses, J.Am.Ceram.Soc.,79 (1996) 681-687.

[17]- Hiromichi Takebe, Yoshikzu Nageno, and Kenji Morinaga. Compositional dependence of Judd-Ofelt parameters in silicate, borate, and phosphate glasses, J. Am. Ceram. Soc.,78 (1995) 1161-1168.

[18]- Yoshikzu Nageno, Hiromichi Takebe, and Kenji Morinaga, Correlation between radiative transition probabilities of Nd^{3+} and composition in silicate,borate, and phosphate, J.Am.Ceram.Soc.,76 (1993) 3081-3086.

[19] T. Ohtsuki,N. Peyghambarian, S. Honkanen, and S.I. Najafi, Gain characterestic of a high concentration Er^{3+} doped phosphate glasse wawguide , J.Appl.Phys.,78 (1995) 3617-3621.

[20]- M.J. Weber, probabilities for radiative and non-radiative decay of Er^{3+} in LaF_3, Phys. Rev., 157 (1966) 262-270.

[21]-D.L. Dexter, and James H. schulman, Theory of concentration quenching in inorganic phosphors, J. Chem. Phys., 22 (1954) 1063-1070.

[22]- B.C. Joshi, and R.Lohani, Non-radiative energy transfer from Tm^{3+} to Ho^{3+} and Nd^{3+} in zinc phosphate glasses, J. Non-Crys. Solids,215 (1997) 103-107.

[23]- B.C. Joshi, and R. Lohani, Non-radiative energy transfer from Dy^{3+} to Ho^{3+} in zinc phosphate glass, J. Non-Crys. Solids, 189, (1995) 242-245.

[24]- B.C. Joshi, M.C. Joshi, Sensitizing Pr^{3+} ions by Tm^{3+} ion phosphate glass, J. Non-Crys. Solids, 142 (1992) 171-174.

Table (2). The measured and calculated line strengths of Er^{3+} doped phosphate glass.

Transition	$S'_{ed}(measured) \times 10^{-21} cm^2$	$S'_{ed}(calculated) \times 10^{-21} cm^2$
$^4I_{15/2} \rightarrow {}^4G_{11/2}$	92.29	92
$^4I_{15/2} \rightarrow {}^4F_{5/2}$	3.67	3.95
$^4I_{15/2} \rightarrow {}^4F_{7/2}$	13.01	13.9
$^4I_{15/2} \rightarrow {}^4S_{3/2}$	4.365	4.035
$^4I_{15/2} \rightarrow {}^4F_{9/2}$	17.7	19.25
$^4I_{15/2} \rightarrow {}^4I_{9/2}$	3.79	2.95
$^4I_{15/2} \rightarrow {}^4I_{11/2}$	7	9

Table (3). Mean absorption wavelength, $\overline{\lambda}$, transition probability per unit time by electric dipole, $\overline{A}_{ed}$, transition probability per unit time by magnetic dipole, $\overline{A}_{md}$, total transition probability per unit time, A , and branching ratio, β for Er^{3+} states in phosphate glass.

SLJ	$S'L'J'$	$\frac{1}{\lambda}(cm^{-1})$	$A_{ed}(s^{-1})$	$A_{md}(s^{-1})$	$A(s^{-1})$	β_R
$^4I_{13/2}$	$^4I_{15/2}$	6542	129.6	33.56	163.16	1
$^4I_{11/2}$	$^4I_{13/2}$	3724	19.31	7.518	157	0.17
	$^4I_{15/2}$	10266	130.71	0		0.8297
$^4I_{9/2}$	$^4I_{11/2}$	2283	0.452	1.075		0.0072
	$^4I_{13/2}$	6007	50.456	0	211.22	0.2388
	$^4I_{15/2}$	12549	159.236	0		0.7544
$^4F_{9/2}$	$^4I_{9/2}$	2812	3.865	2.141		0.0004
	$^4I_{11/2}$	5095	41.765	5.273	1546.15	0.0304
	$^4I_{13/2}$	8819	80.936	0		0.0523
	$^4I_{15/2}$	15361	1412.17	0		0.9133
$^4S_{3/2}$	$^4F_{9/2}$	3052	0.286	0		0.00012
	$^4I_{9/2}$	5864	16.67	0		0.0072
	$^4I_{11/2}$	8147	40.314	0	2298.77	0.0175
	$^4I_{13/2}$	11871	615.169	0		0.2676
	$^4I_{15/2}$	18413	1626.34	0		0.7074
$^4G_{11/2}$	$^2H_{11/2}$	7250	31.71	9.716		0.00074
	$^4F_{9/2}$	11094	875	2.431		0.0158
	$^4I_{9/2}$	13906	291.28	0.543	55540.3	0.0052
	$^4I_{11/2}$	16189	744.56	0.1		0.0134
	$^4I_{13/2}$	19913	15710.8	40.43		0.2836
	$^4I_{15/2}$	26455	37833.7	0		0.681

Table (4). The measured and calculated line strengths of Er^{3+} in borate glass.

Transition	$S'_{ed}(measured) \times 10^{-21} cm^2$	$S'_{ed}(calculated) \times 10^{-21} cm^2$
$^4I_{15/2} \rightarrow {}^4G_{11/2}$	43.321	45
$^4I_{15/2} \rightarrow {}^4F_{5/2}$	0.836	0.69
$^4I_{15/2} \rightarrow {}^4F_{7/2}$	7.22	2.322
$^4I_{15/2} \rightarrow {}^4S_{3/2}$	4.7793	6.84
$^4I_{15/2} \rightarrow {}^2H_{11/2}$	26.5	35
$^4I_{15/2} \rightarrow {}^2H_{9/2}$	2.826	1.83
$^4I_{15/2} \rightarrow {}^4F_{9/2}$	10.735	11
$^4I_{15/2} \rightarrow {}^4I_{9/2}$	1.1641	2.46

Table (5). Mean absorption wavelength, $\overline{\lambda}$, transition probability per unit time by electric dipole, $\overline{A}_{ed}$, transition probability per unit time by magnetic dipole, $\overline{A}_{md}$, total transition probability per unit time, A , and branching ratio, β for Er^{3+} states in borate glass.

SLJ	$S'L'J'$	$\frac{1}{\lambda}(cm^{-1})$	$A_{ed}(s^{-1})$	$A_{md}(s^{-1})$	$A(s^{-1})$	β_R
$^4I_{13/2}$	$^4I_{15/2}$	6527	31.5	33.56	65.06	1
$^4I_{11/2}$	$^4I_{13/2}$	3718	4.5	7.518	157.5	0.17
	$^4I_{15/2}$	10250	40.5	0		0.8297
$^4I_{9/2}$	$^4I_{11/2}$	2280	0.452	1.075		0.0248
	$^4I_{13/2}$	6000	9.8	0	61.427	0.1595
	$^4I_{15/2}$	12530	50.1	0		0.8156
$^4F_{9/2}$	$^4I_{9/2}$	2810	1.501	2.141		0.0038
	$^4I_{11/2}$	5090	16.21	5.273	935.5	0.0229
	$^4I_{13/2}$	8810	42.3	0		0.045
	$^4I_{15/2}$	15340	868	0		0.927833
$^4S_{3/2}$	$^4F_{9/2}$	3050	0.286	0	289.45	0.00012
	$^4I_{9/2}$	5859	17.89	0		0.0072
	$^4I_{11/2}$	8140	7.15	0		0.0175
	$^4I_{13/2}$	11850	232.5	0		0.2676
	$^4I_{15/2}$	18413	1626.34	0		0.7074
$^4G_{11/2}$	$^2H_{11/2}$	7250	24	9.716		0.0014
	$^4F_{9/2}$	11080	484.182	2.431		0.0114
	$^4I_{9/2}$	13906	649	0.543	22700.9	0.0063
	$^4I_{11/2}$	16150	649	0.1		0.0286
	$^4I_{13/2}$	19900	1391	40.43		0.064
	$^4I_{15/2}$	26420	19954.7	0		0.879

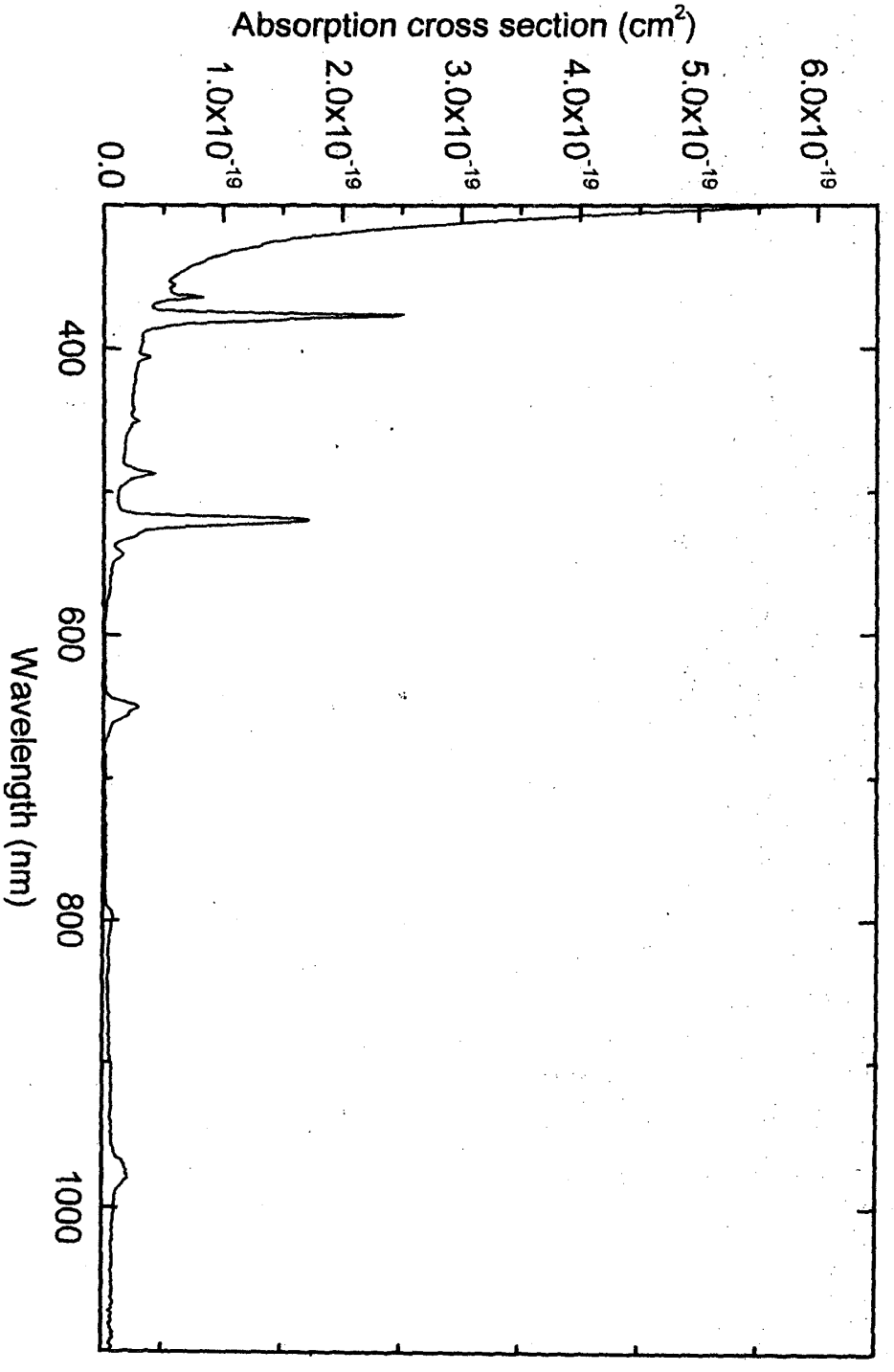
Absorption cross section (cm²)
0.0
1.0x10⁻¹⁹
2.0x10⁻¹⁹
3.0x10⁻¹⁹
4.0x10⁻¹⁹
5.0x10⁻¹⁹
6.0x10⁻¹⁹
Wavelength (nm)
400
600
800
1000

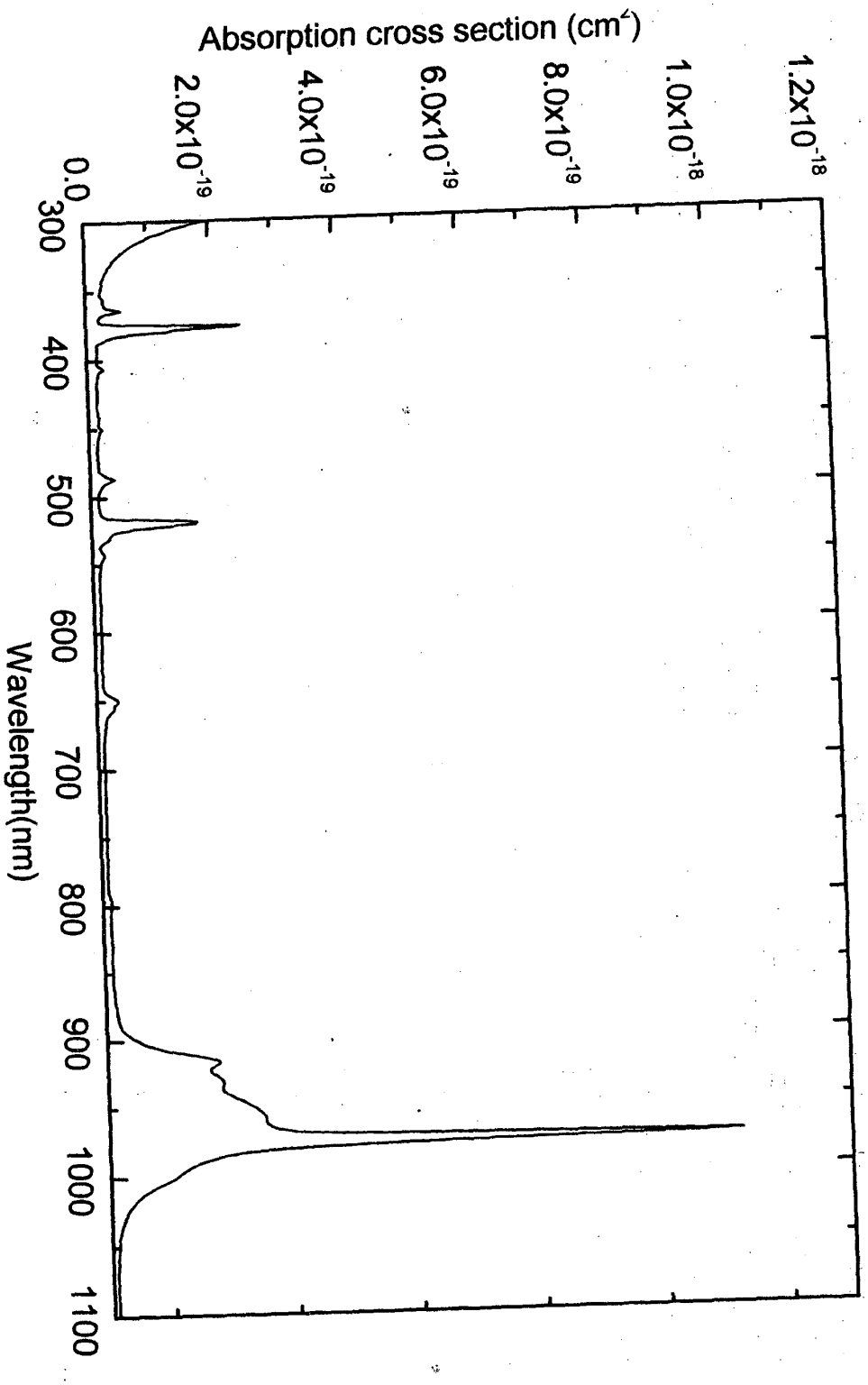
Absorption cross section (cm²)
0.0
2.0x10⁻¹⁹
4.0x10⁻¹⁹
6.0x10⁻¹⁹
8.0x10⁻¹⁹
1.0x10⁻¹⁸
1.2x10⁻¹⁸
300
400
500
600
700
800
900
1000
1100
Wavelength(nm)

Fig.

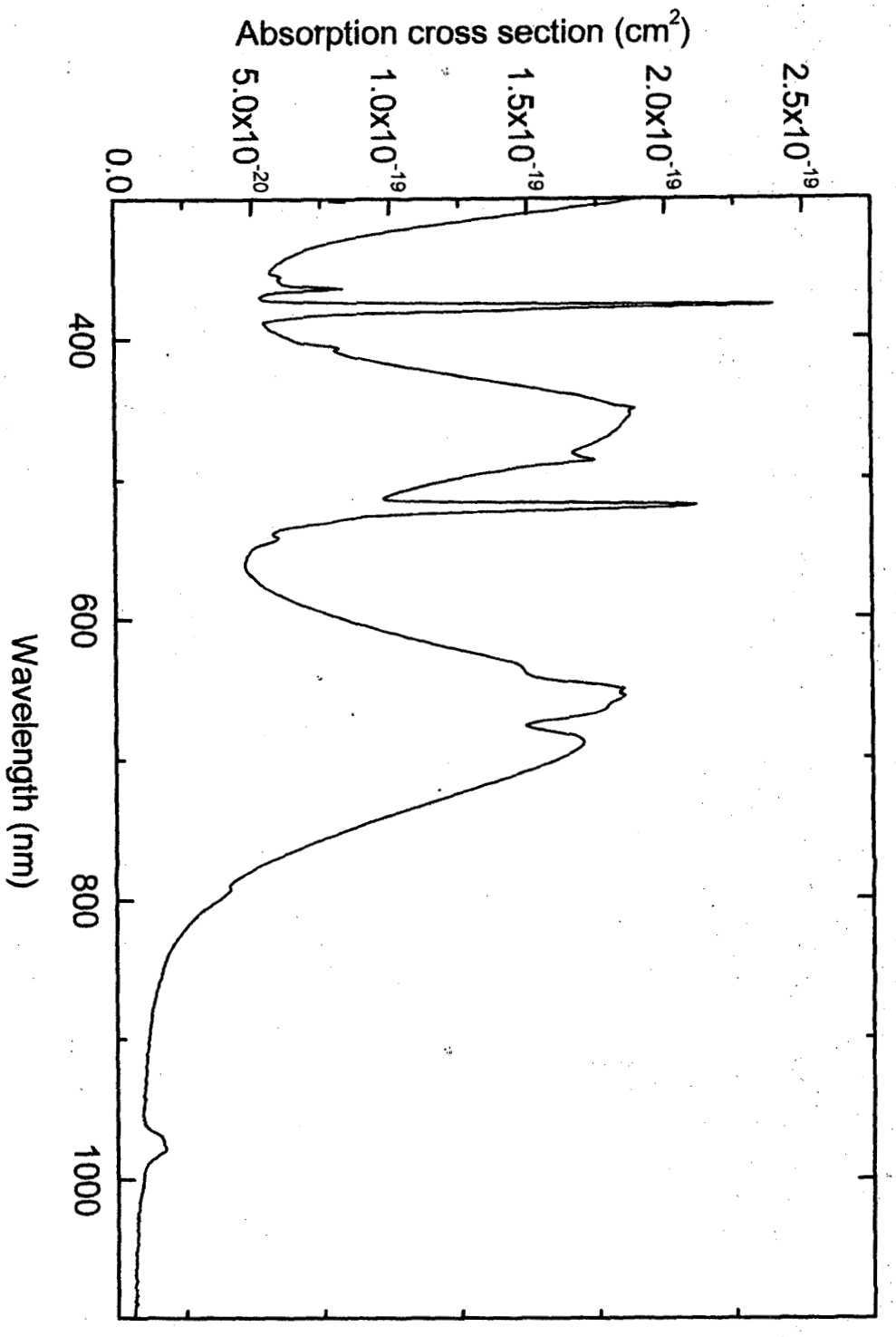
Absorption cross section (cm^2)
0.0
5.0x10^{-20}
1.0x10^{-19}
1.5x10^{-19}
2.0x10^{-19}
2.5x10^{-19}
400
600
800
1000
Wavelength (nm)

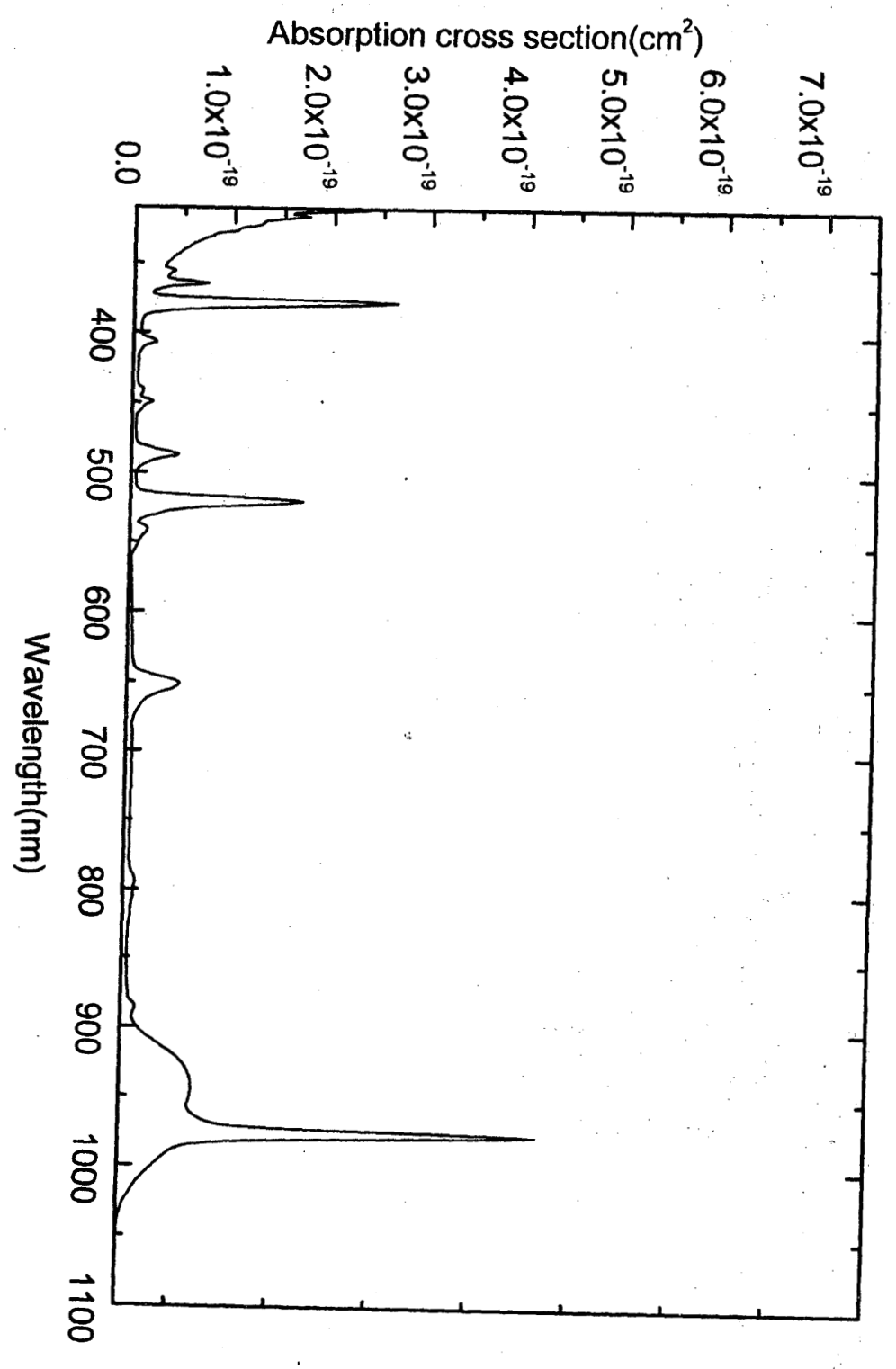
Absorption cross section(cm^2)
0.0
1.0x10^{-19}
2.0x10^{-19}
3.0x10^{-19}
4.0x10^{-19}
5.0x10^{-19}
6.0x10^{-19}
7.0x10^{-19}
Wavelength(nm)
400
500
600
700
800
900
1000
1100

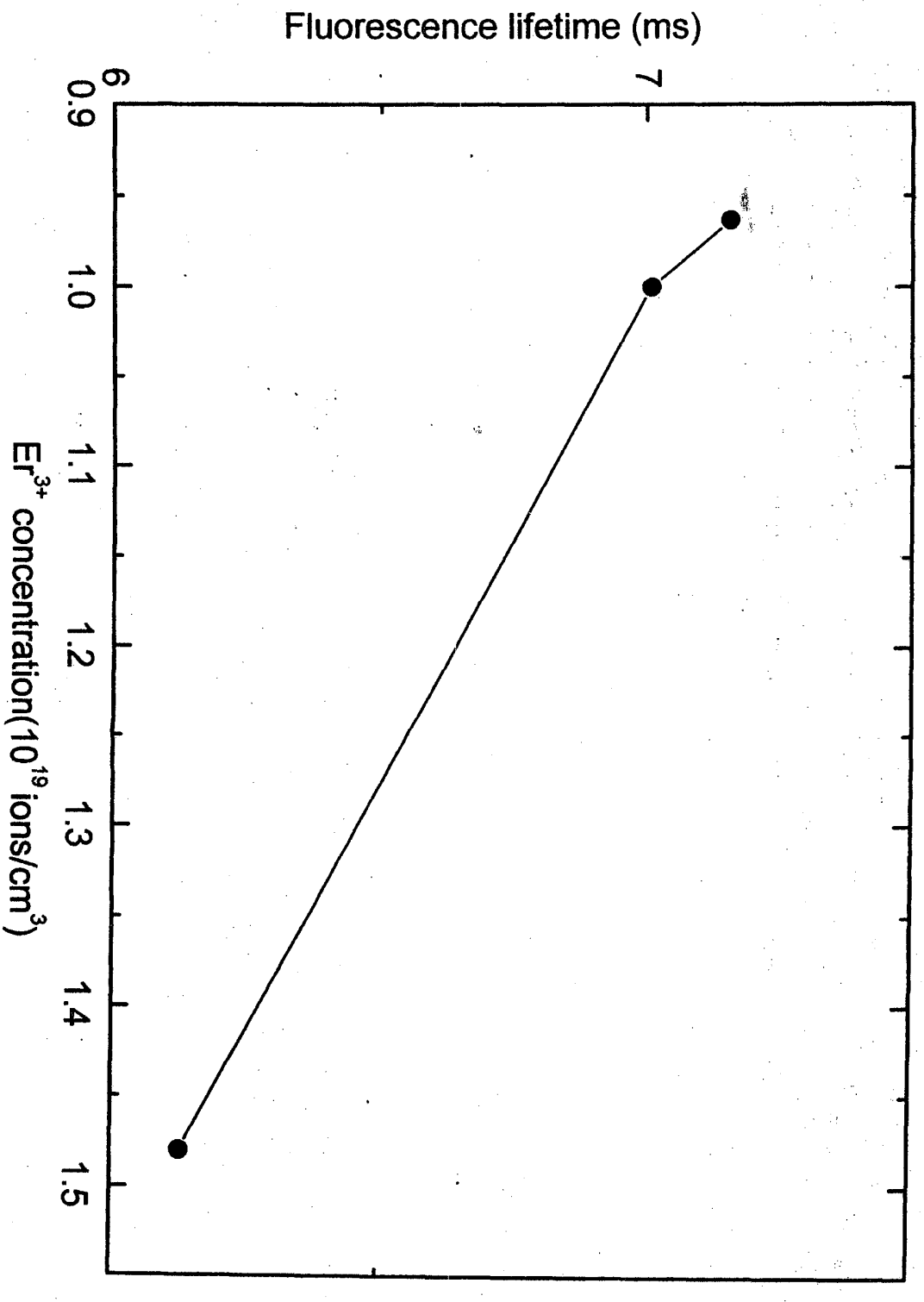
Fluorescence lifetime (ms)
6
7
0.9
1.0
1.1
1.2
1.3
1.4
1.5
Er3+ concentration(10^19 ions/cm^3)

Fig. 2

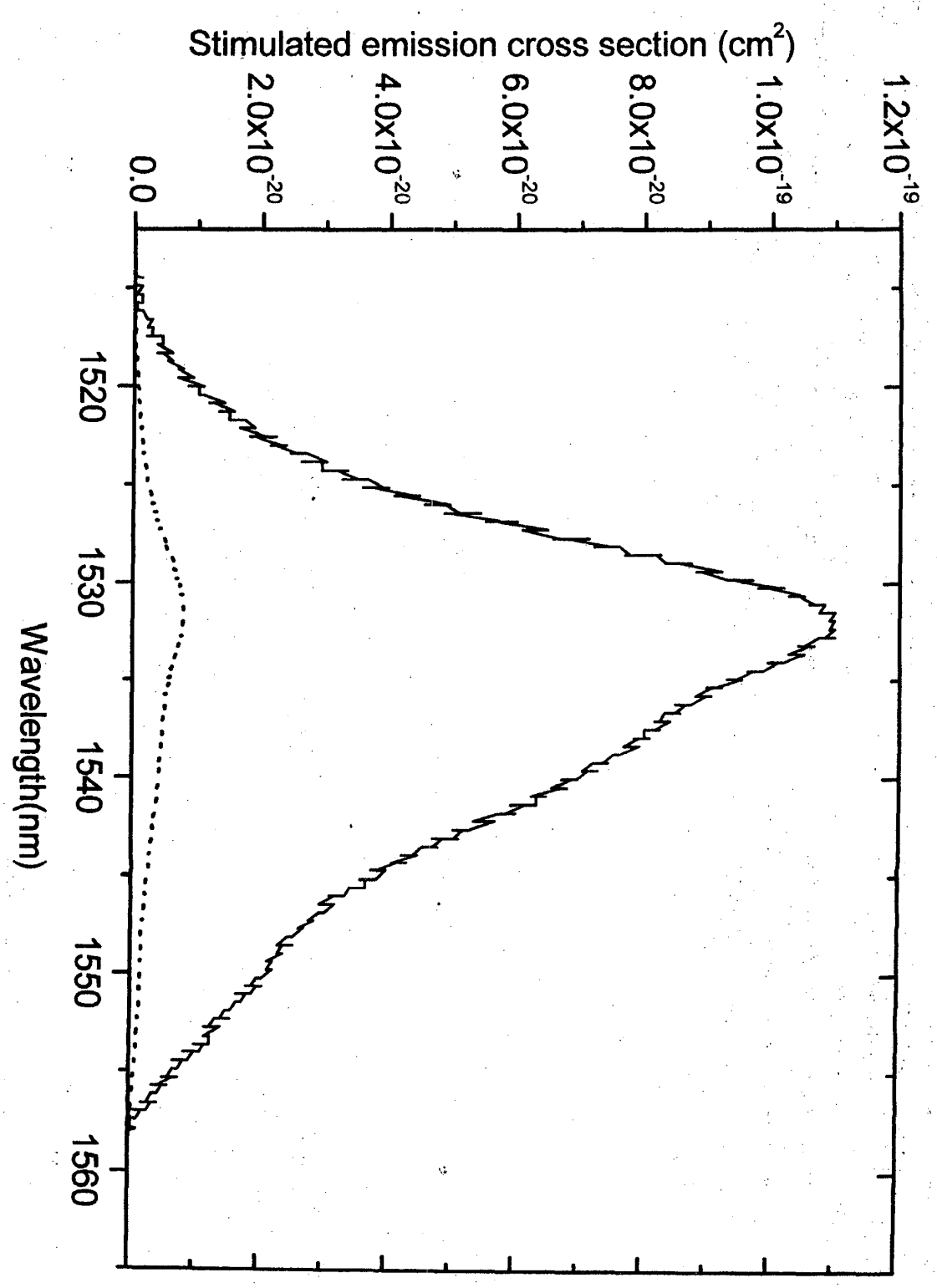
Stimulated emission cross section (cm^2)
0.0
2.0x10^{-20}
4.0x10^{-20}
6.0x10^{-20}
8.0x10^{-20}
1.0x10^{-19}
1.2x10^{-19}
1520
1530
1540
1550
1560
Wavelength(nm)

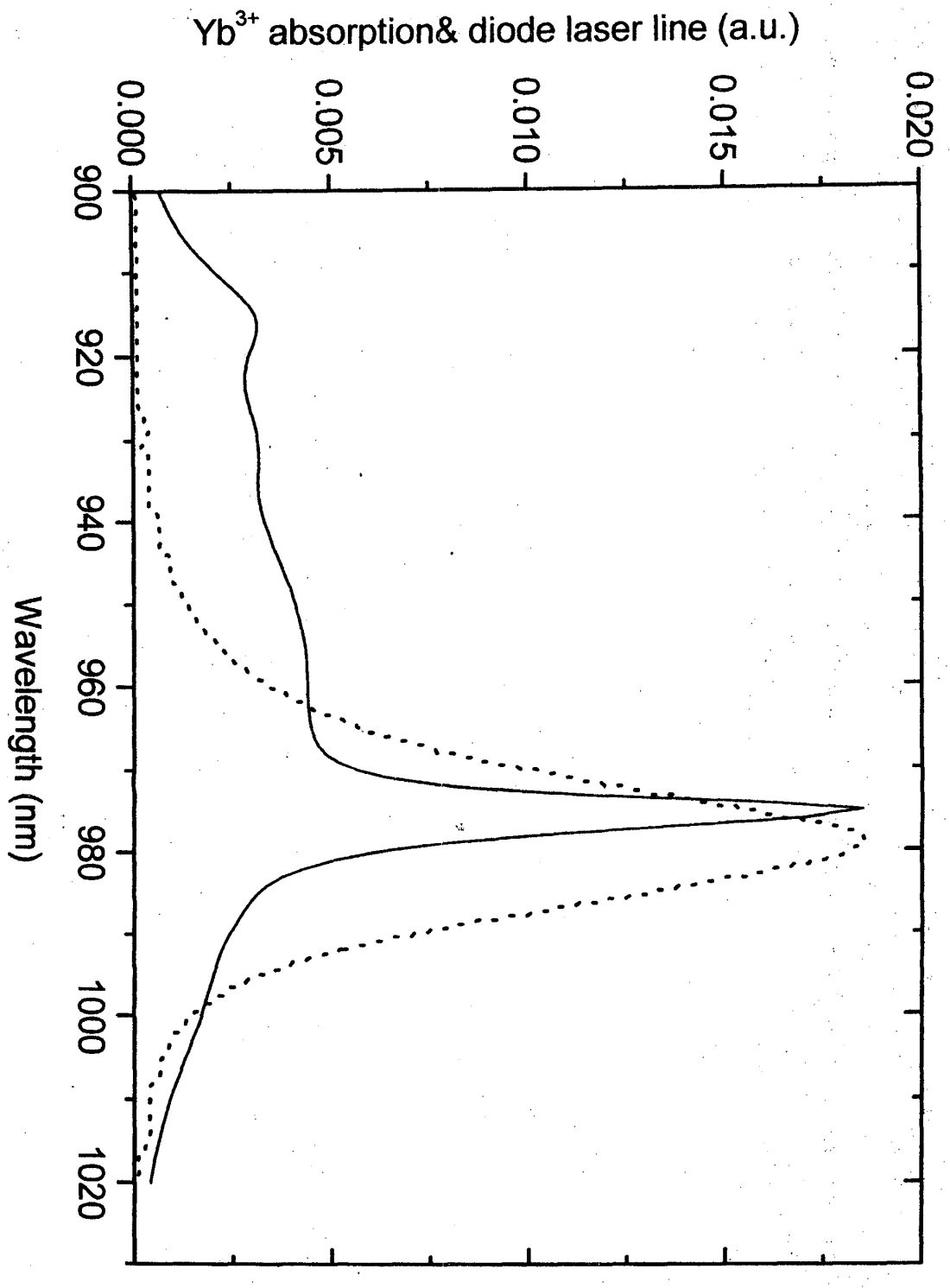
Yb3+ absorption& diode laser line (a.u.)
0.000
0.005
0.010
0.015
0.020
900
920
940
960
980
1000
1020
Wavelength (nm)

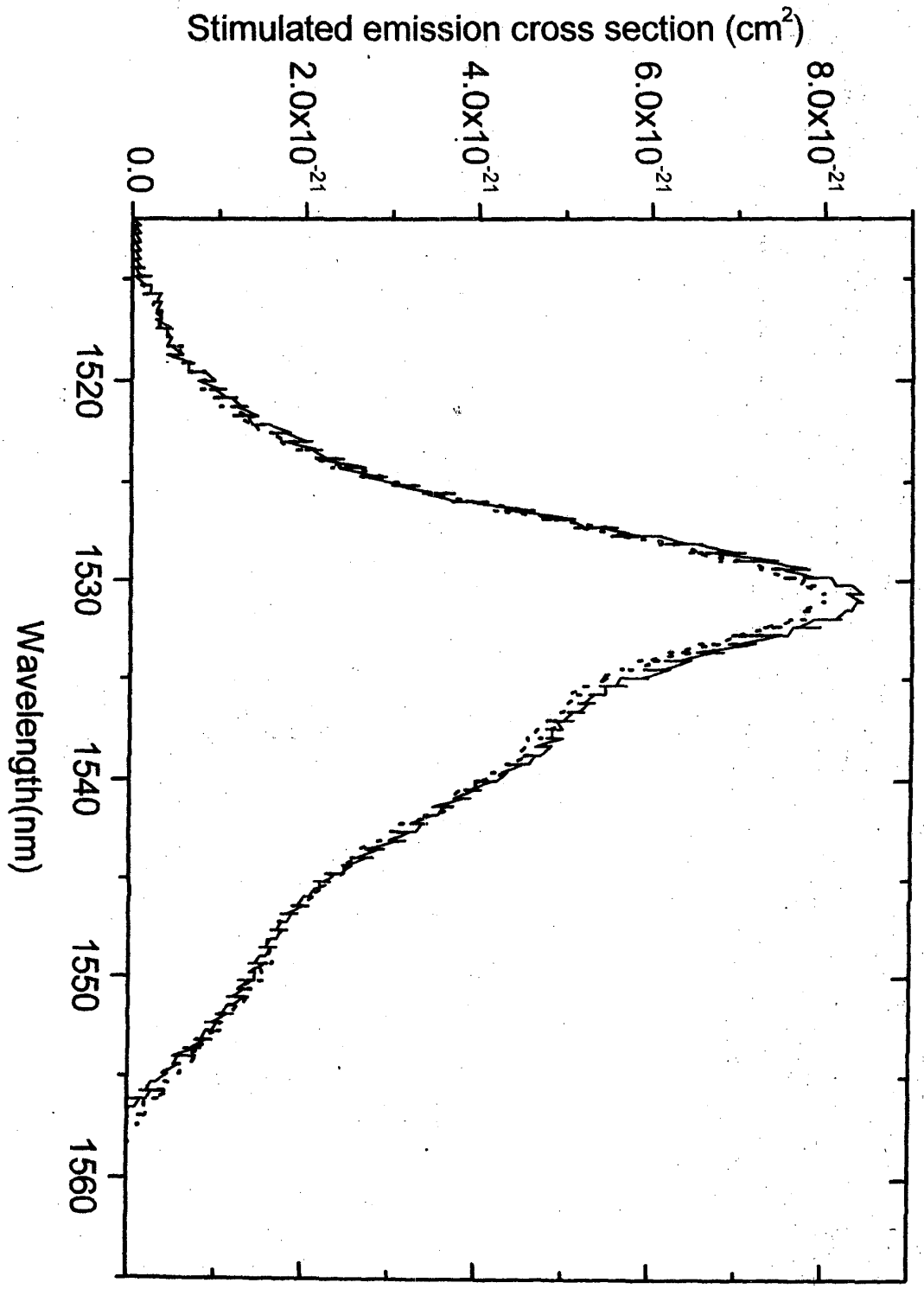
Stimulated emission cross section (cm^2)
0.0
2.0x10^{-21}
4.0x10^{-21}
6.0x10^{-21}
8.0x10^{-21}
Wavelength(nm)
1520
1530
1540
1550
1560

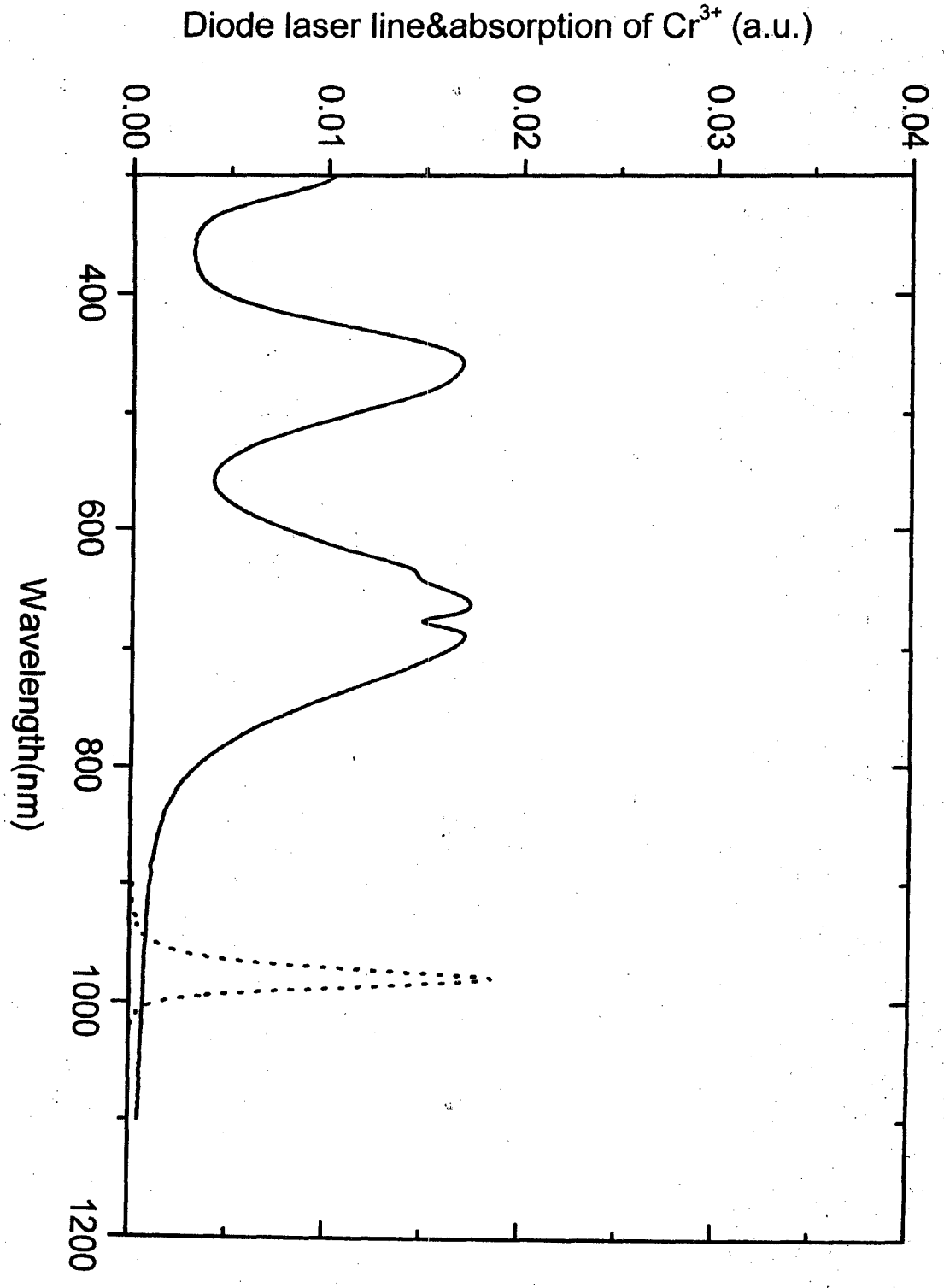
Diode laser line&absorption of Cr^{3+} (a.u.)
0.00
0.01
0.02
0.03
0.04
400
600
800
1000
1200
Wavelength(nm)

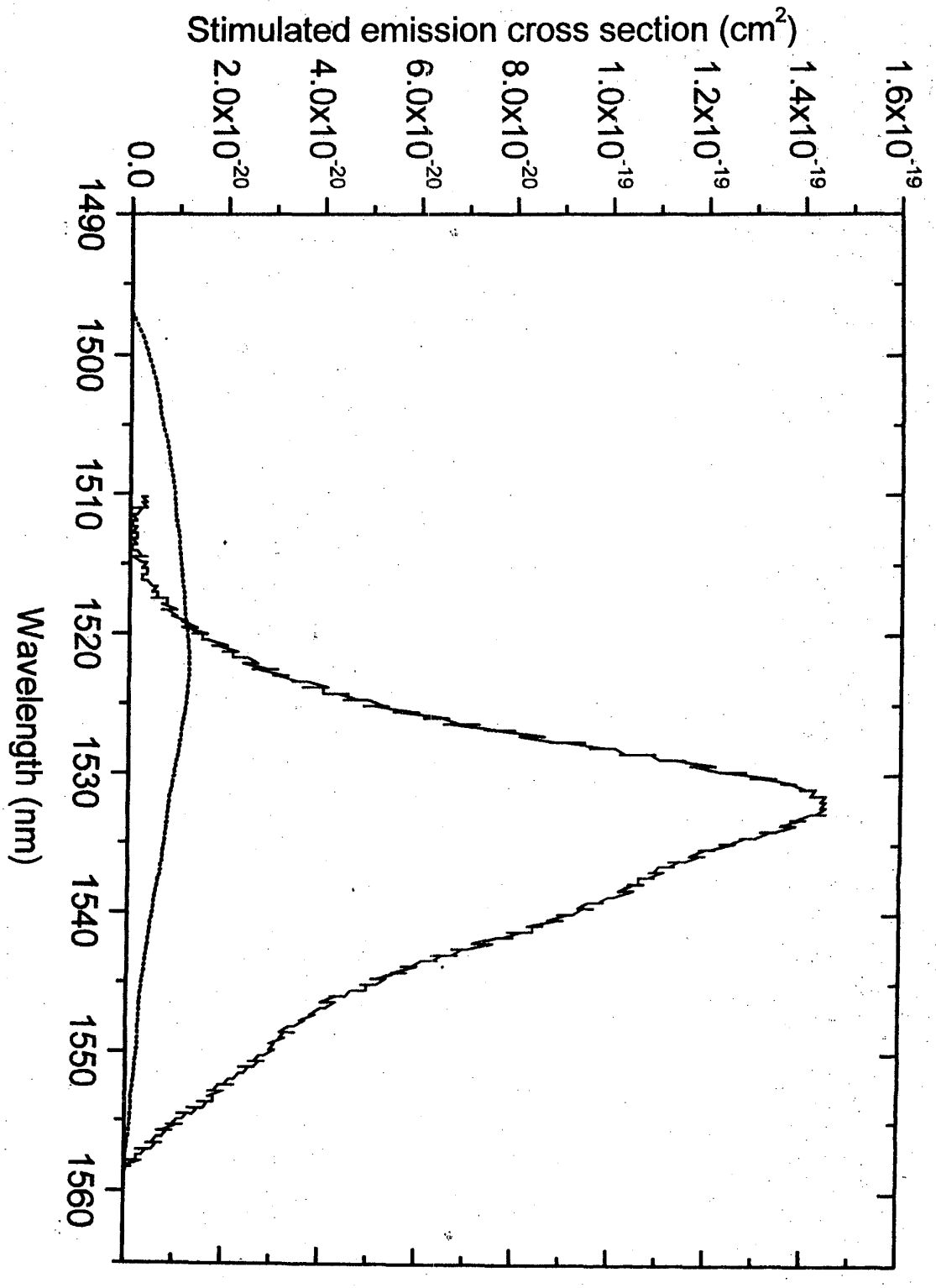
Stimulated emission cross section (cm^2)
0.0
2.0x10^{-20}
4.0x10^{-20}
6.0x10^{-20}
8.0x10^{-20}
1.0x10^{-19}
1.2x10^{-19}
1.4x10^{-19}
1.6x10^{-19}
Wavelength (nm)
1490
1500
1510
1520
1530
1540
1550
1560

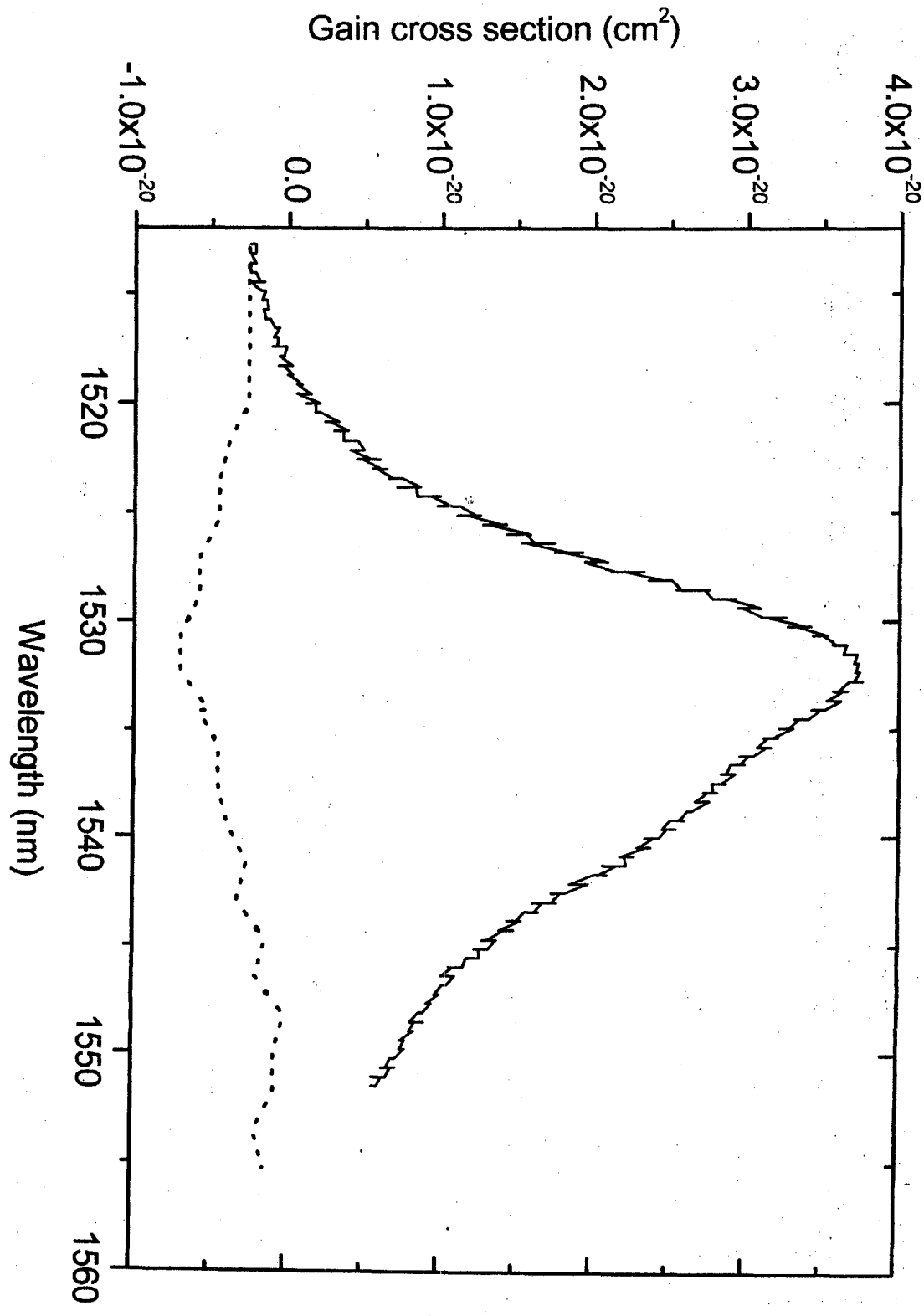
Gain cross section (cm^2)
-1.0x10^{-20}
0.0
1.0x10^{-20}
2.0x10^{-20}
3.0x10^{-20}
4.0x10^{-20}
1520
1530
1540
1550
1560
Wavelength (nm)

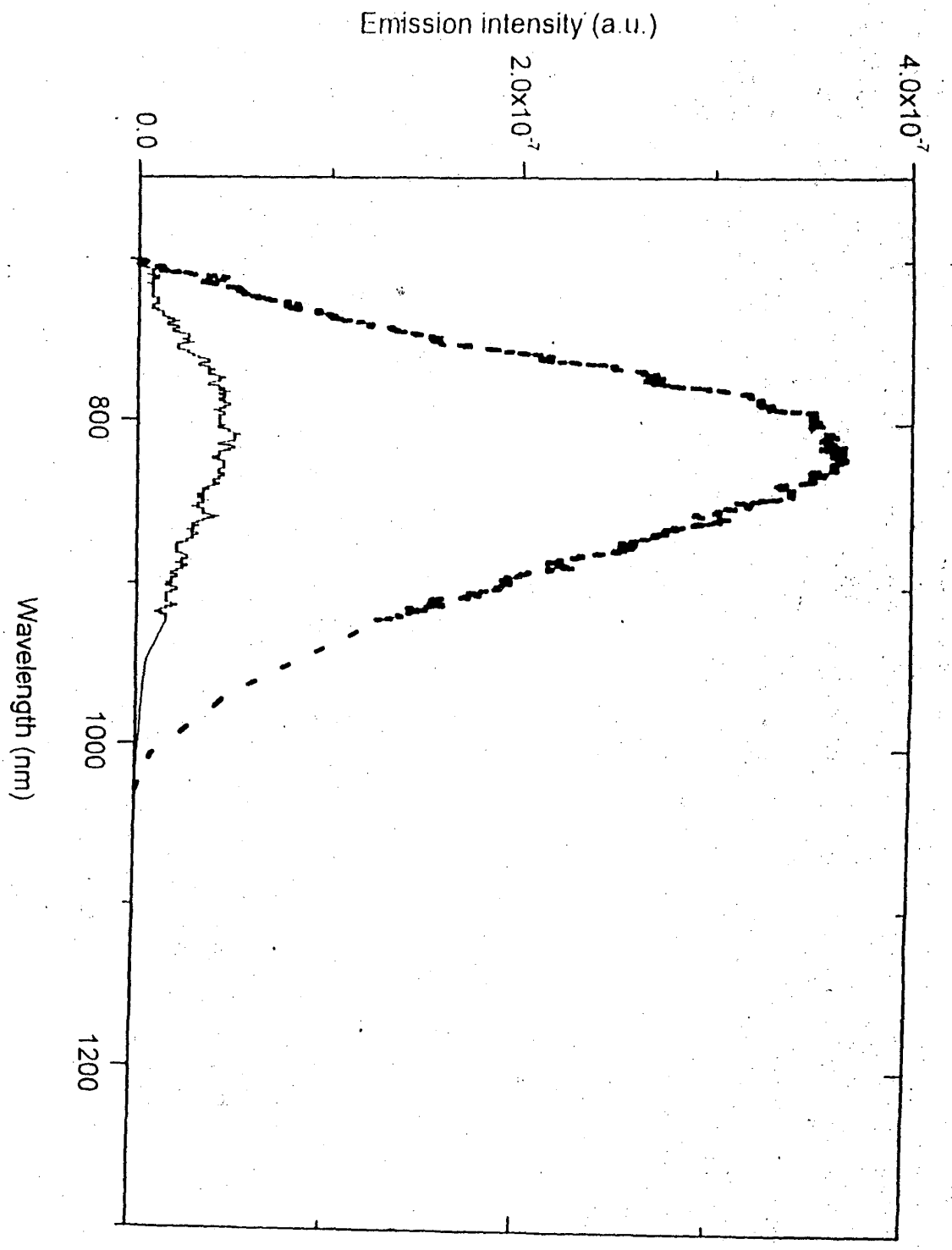
Emission intensity (a.u.)
0.0
2.0x10^{-7}
4.0x10^{-7}
800
1000
1200
Wavelength (nm)

Figure captions

Fig.1(a).Absorption spectrum of Er^{3+} doped phosphate glass. Er^{3+} concentration is 0.0495 mol.%,sample thickness is 2 mm.

Fig.1(b). Absorption spectrum of Er^{3+} :Yb^{3+} doubly doped in phosphate glass. Er^{3+} concentration is 0.0495 mol.%, and Yb^{3+} concentration is 2.445 mol.%. Sample thickness is 2 mm.

Fig.1(c). Absorption spectrum of Er^{3+}: Cr^{3+} doubly doped in phosphate glass. Er^{3+} concentration is 0.0495 mol.%, and Cr^{3+} concentration is 0.082 mol.%. Sample thickness is 2 mm.

Fig.1(d). Absorption spectrum of Er^{3+}:Yb^{3+} doubly doped in borate glass. Er^{3+} concentration is 0.0165 mol.%, and Yb^{3+} concentration is 1.785. Sample thickness is 2 mm.

Fig. 2. Concentration quenching of Er^{3+} in lithium aluminum phosphate glass.

Fig.3. Effect of Yb^{3+} as a sensitizer on the stimulated emission cross section of Er^{3+} at 1534. (....) Er^{3+} singly-doped, and (—) Er^{3+}:Yb^{3+} doubly-doped in phosphate glass.

Fig. 4. Matching between Yb^{3+} absorption and laser line. (....). Diode laser line, and (—) Yb^{3+} absorption in phosphate glass.

Fig. 5.Effect of Cr^{3+} as a sensitizer on the stimulated emission cross section of Er^{3+} at 1534 nm. (....) Er^{3+} singly-doped, and (—) Er^{3+}:Cr^{3+} doubly-doped in phosphate glass.

Fig. 6. Mismatching between Cr^{3+} absorption bands and diode laser line at 980 nm. (....) Diode laser line, and (—) Cr^{3+} absorption in phosphate glass.

Fig. 7. Comparison between phosphate and borate as hosts for Er^{3+}:Yb^{3+} co-doped. (....) Er^{3+}:Yb^{3+}doubly-doped in borate glass , and (——) Er^{3+}:Yb^{3+} doubly-doped in phosphate glass.

Fig. 8. Effect of Yb^{3+} as a sensitizer on the gain cross-section of Er^{3+} at 1534 nm. (....) Er^{3+} singly-doped, and (——) Er^{3+}:Yb^{3+} doubly-doped in phosphate glass.

Fig. 9. Transfer of population from Cr^{3+} to Er^{3+} (....)Fluorescence of Cr^{3+} singly-doped, and (——) Cr^{3+}:Er^{3+} doubly-doped.